Assignment 2 – In-plane Finite Element Model of a Truss Bridge

Prof. R. Corradi, Dr. I. La Paglia

Contents

1) FE model of the structure

The first step in the definition of a finite element model is the mesh generation, this implies dividing the structure in an adequate number of finite elements (FEs) by placing nodes in correspondence of geometry or property discontinuities.

The finite elements must be defined such that they are operating in their quasi-static region, therefore, the first natural frequency of each one of them must be higher than the maximum frequency of interest. Each finite element is assumed to be a pinned-pinned beam since the analytical formula to compute the natural frequencies is available; to account for the fact that in the real structure the FEs might not be pinned-pinned beams, a safety margin is considered. Indeed, it has been imposed that the first natural frequency of each FE must be at least 1.5 times greater than the maximum frequency of interest.

In this case the frequency range of interest yields between $0\ Hz \div 7\ Hz$ ($\Omega_{max} = 2\pi * 7\ \ rad/s$). Starting from the analytical expression for the first natural frequency of a pinned-pinned beam and imposing $\omega_k^{(1)} \geq 1.5 * \ \Omega_{max}$, the expression for the maximum allowed length of each k-finite element can be derived:

$$L_{max,k} = \sqrt{\left(\frac{\pi^2}{1.5 * \Omega_{max}} \sqrt{\frac{EJ}{m}}\right)}$$

This formula suggests that the maximum length of the FEs depends also on the physical properties of the structure itself. Note that the bridge is composed of a lower deck, six different types of diagonal members and two types of upper chord elements; for this reason, nine different $L_{max,k}$ have been computed; among this set of values, the lowest one was considered as limiting constraint ($min(L_{max,k}) = 7.8886\ m$). The mesh has been generated by placing a node in the middle point of each bridge element, as can be seen in Fig.1.

Since the length of each finite element L_k happens to be lower than $7.8886\ m$, the selected mesh is suitable to study the vibration modes up to $7\ Hz$.

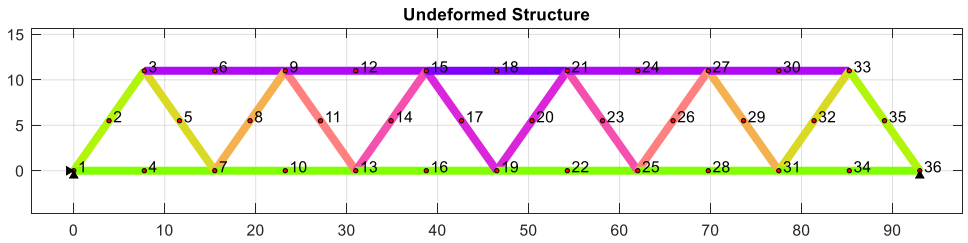

Figure 1: nodes enumeration

2) Natural frequencies and mode shapes

To compute the natural frequency, we first determined the mass and stiffness matrices of the system. These matrices were then partitioned into four submatrices: free-free, free-constrained, constrained-free, and constrained-constrained.

To calculate the natural frequencies, we based the code on the eigenvalue problem. Specifically, we used the ***eig*** function to compute the eigenvalues and eigenvectors of the matrix obtained by multiplying the inverse of the free-free mass matrix by the free-free stiffness matrix.

Finally, the resulting eigenvalues and eigenvectors were arranged in ascending order using the ***sort*** function, ensuring that the natural frequencies were organized from the smallest to the largest.

Here the plots of the mode shapes up to the sixth one, as requested by the assignment, using a scale factor of 1.5.

	Mode 1	Mode 2	Mode 3	Mode 4	Mode 5	Mode 6
ω	15,8190	32,9057	34,9432	35,6091	40,1835	43,1370

Figure 1 First six natural frequencies

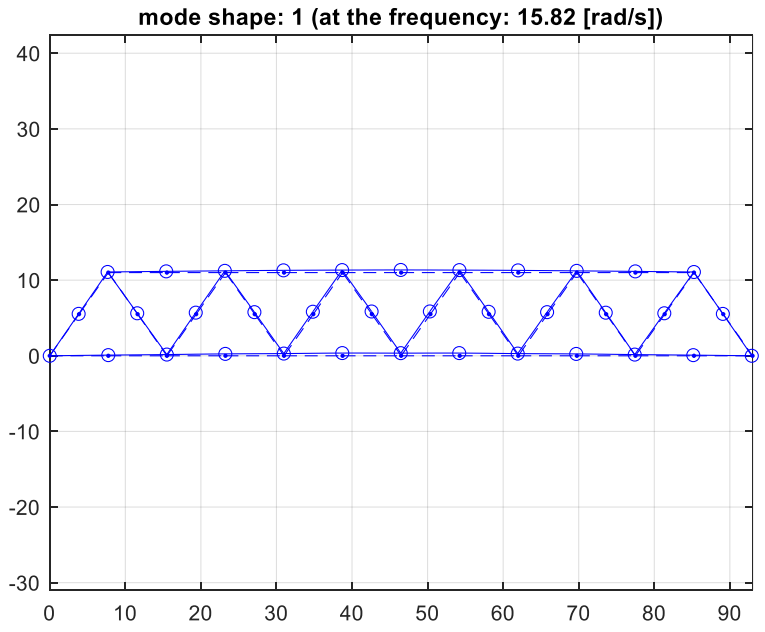

Figure 2 Mode shape 1

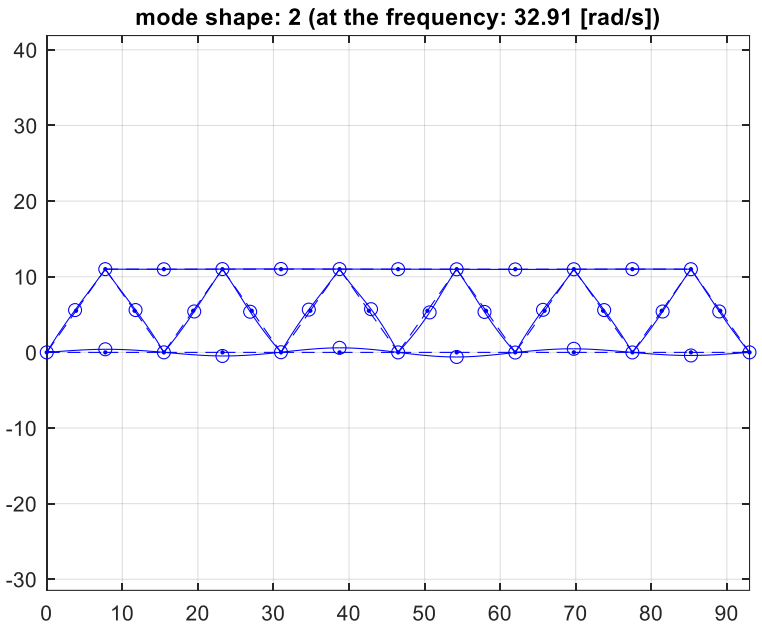

Figure 3 Mode shape 2

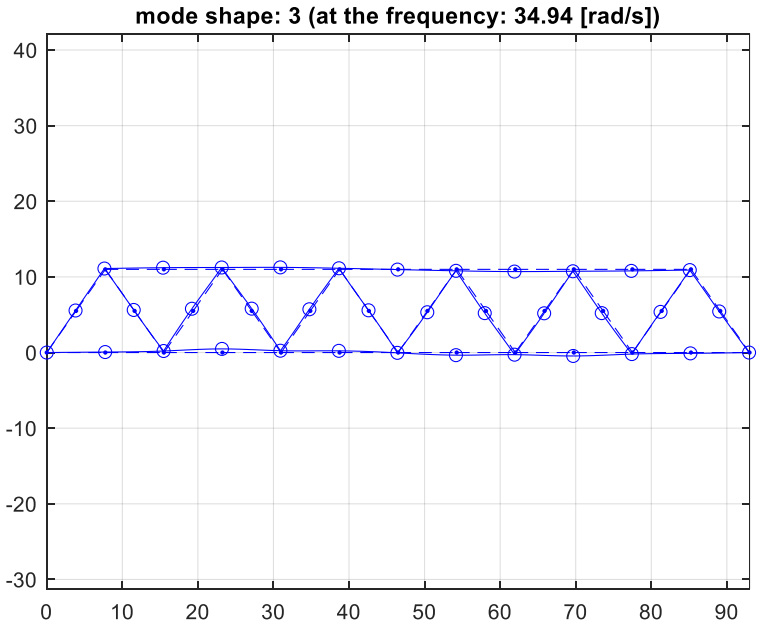

Figure 4 Mode shape 3

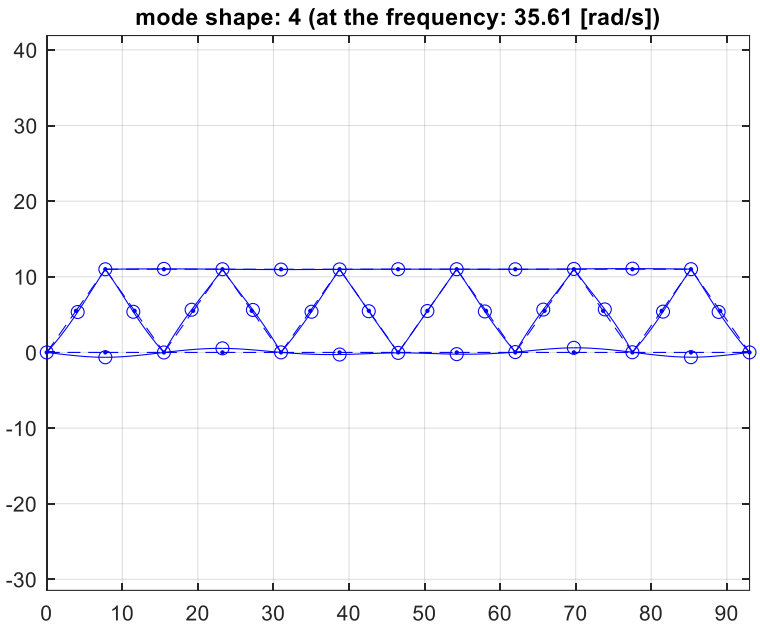

Figure 5 Mode shape 4

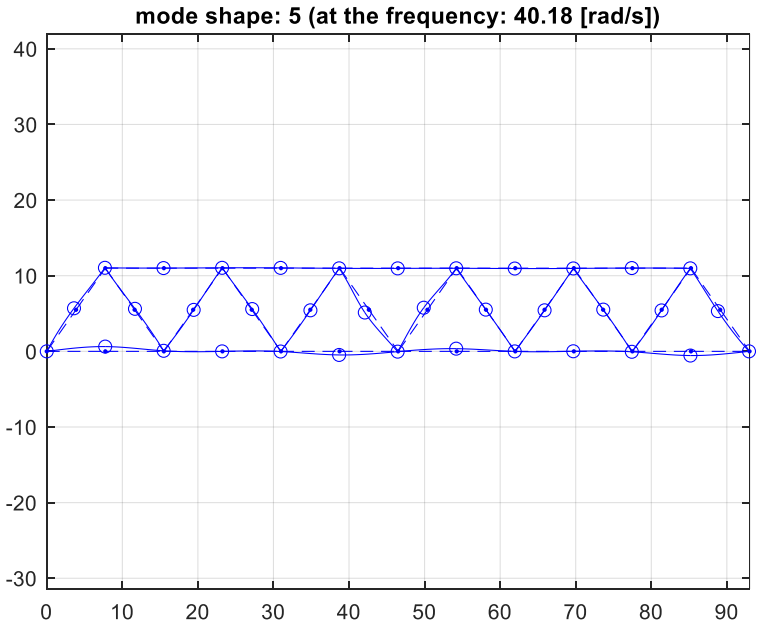

Figure 6 Mode shape 5

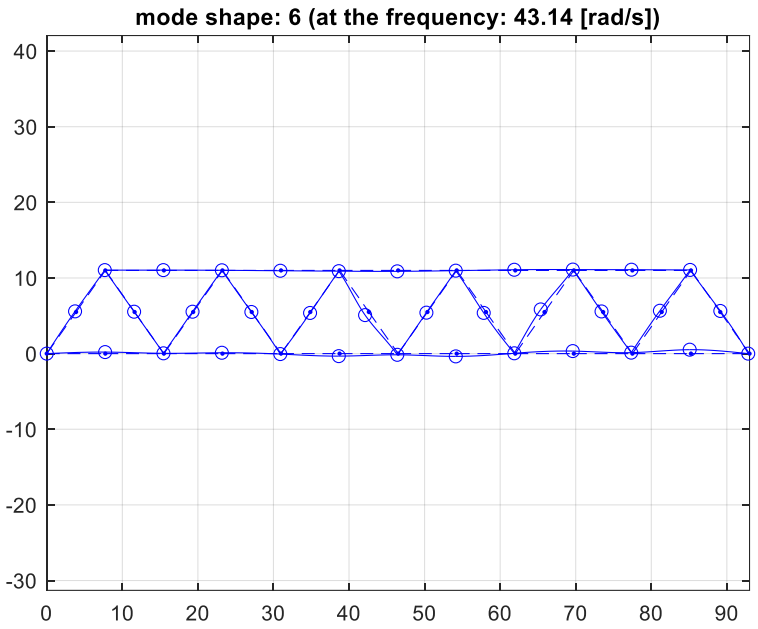

Figure 7 Mode shape 6

3) Damping matrix

To compute the damping matrix, we used the values of ξ provided in the assignment and determined the corresponding α and β coefficients required for its calculation.

Initially, we constructed vector B, which contains the two given values of ξ, and assembled the matrix A as shown below, based on the first two frequencies:

$$[A] = \begin{bmatrix} \frac{1}{2\omega_1} & \frac{\omega_1}{2} \\ \frac{1}{2\omega_2} & \frac{\omega_2}{2} \end{bmatrix}$$

Then we computed the two coefficients through a least square error minimization:

$$\begin{bmatrix} \alpha \\ \beta \end{bmatrix} = ([A]^T[A])^{-1}[A]^T\underline{B}$$

And we obtained α = 0.2631 and β = 2.1285e-04.

So finally, we computed the damping matrix

$$[C_{FF}] = \alpha[M_{FF}] + \beta[K_{FF}]$$

4) FRFs related to an input force

4.a) Vertical displacements and vertical accelerations

To obtain the FRF for a vertical force applied in the node A we built the corresponding force vector. We considered a vector with zero in every element except from the DoF corresponding to the vertical displacement of the node A, where we applied a unitary force. We found the number of the specific DoF using the ***idb*** function.

$$\underline{F_0} = \{0 \dots \ 0\ 1\ 0 \dots 0\}^T$$

Vertical displacement

Then, we only needed to solve this simple system

$$(-\Omega^2[M_{FF}] + j\Omega[C_{FF}] + [K_{FF}])\underline{X}e^{j\Omega t} = \underline{F_0}e^{j\Omega t}$$

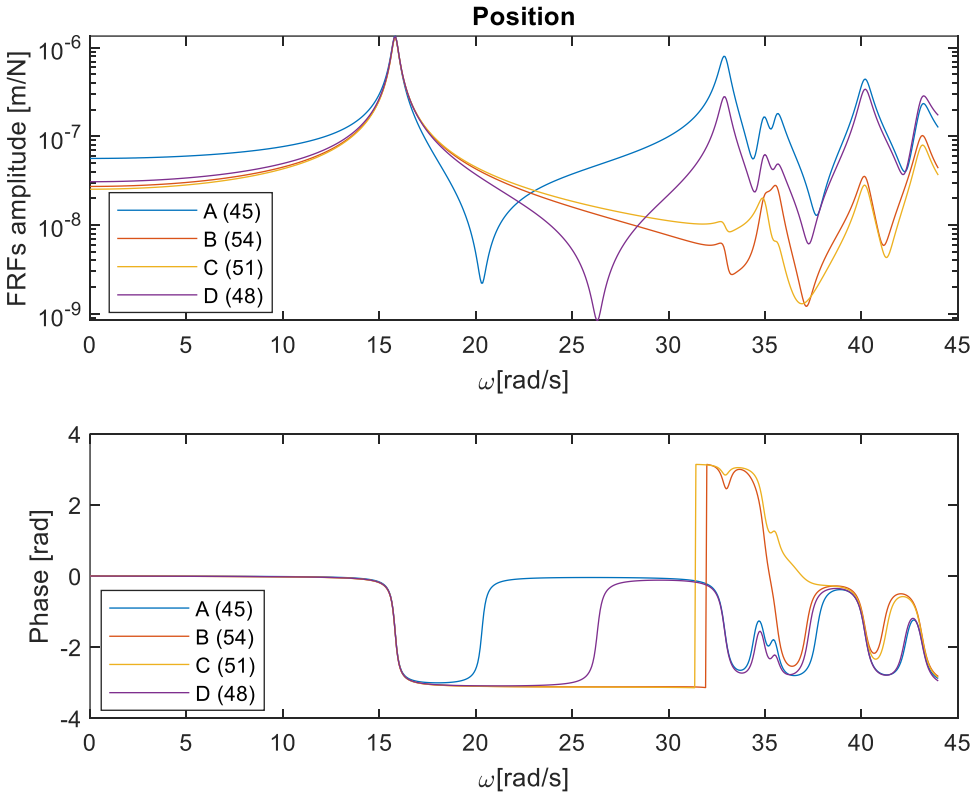

Figure 8

Some observations can be made over the previous plot:

- A (node 16)
  - It is a collocated FRF: sequence of resonance and antiresonance can be seen
  - All modes can be observed
- B (node 19)
  - Mode 2 is not observable because point B is a node for that vibration mode
  - Mode 3 is barely observable because point B is very close to a node
  - Mode 4 is also barely observable, not because of the proximity with a node but because the vibration is low

- C (node 18)
    - Overall similar behavior of the FRF of point B, only difference is that mode 4 is not observable
- D (node 17)
    - Modes 1 and 2 are observable
    - Mode 3 and 4 are observables but the amplitude of the vibration is lower compared to the one in point A
    - Mode 5 and 6 are observables

Vertical accelerations

To compute the FRFs for the vertical acceleration, we multiplied the position vector obtained for the frequency squared.

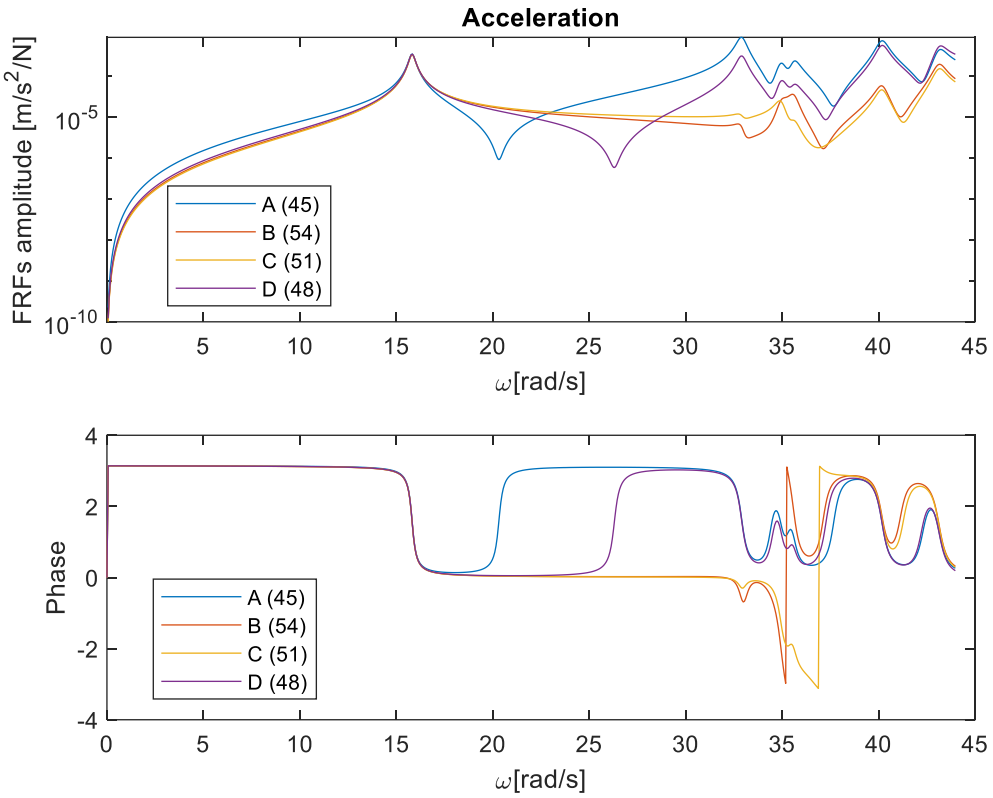

Figure 9

4.b) Internal forces

From the FE formulation, axial and transversal displacement are given as a function of the nodal displacement though the shape functions defined in the local reference system.

$$u(\xi, t) = a + b\xi$$

$$w(\xi, t) = a + b\xi + c\xi^2 + d\xi^3$$

Considering the Euler-Bernoulli beam:

$$N = EA\frac{\partial u}{\partial \xi} \qquad M = EJ\frac{\partial^2 w}{\partial \xi^2} \qquad T = EJ\frac{\partial^3 w}{\partial \xi^3}$$

Assuming the shape functions for axial deformation as a linear function of ξ:

$$u(\xi, t) = a + b\xi \quad \Rightarrow \quad \begin{cases} a = x_i^L \\ b = \dfrac{x_j^L - x_i^L}{L_k} \end{cases}$$

Assuming the shape functions for bending deformation as a cubic function of ξ:

$$w(\xi, t) = a + b\xi + c\xi^2 + d\xi^3 \quad \Rightarrow \quad \begin{cases} a = y_i^L \\ b = \theta_i^L \\ c = -\dfrac{3}{L_k^2}y_i^L + \dfrac{3}{L_k^2}y_j^L - \dfrac{2}{L_k}\theta_i^L - \dfrac{1}{L_k}\theta_j^L \\ d = \dfrac{2}{L_k^3}y_i^L - \dfrac{2}{L_k^3}y_j^L + \dfrac{1}{L_k^2}\theta_i^L + \dfrac{1}{L_k^2}\theta_j^L \end{cases}$$

Then, the internal are easily computed

$N = EA\dfrac{\partial u}{\partial \xi}$	$M = EJ\dfrac{\partial^2 w}{\partial \xi^2}$	$T = EJ\dfrac{\partial^3 w}{\partial \xi^3}$
$\dfrac{\partial u}{\partial \xi} = b$	$\dfrac{\partial^2 w}{\partial \xi^2} = 2c + 6d\xi$	$\dfrac{\partial^3 w}{\partial \xi^3} = 6d$

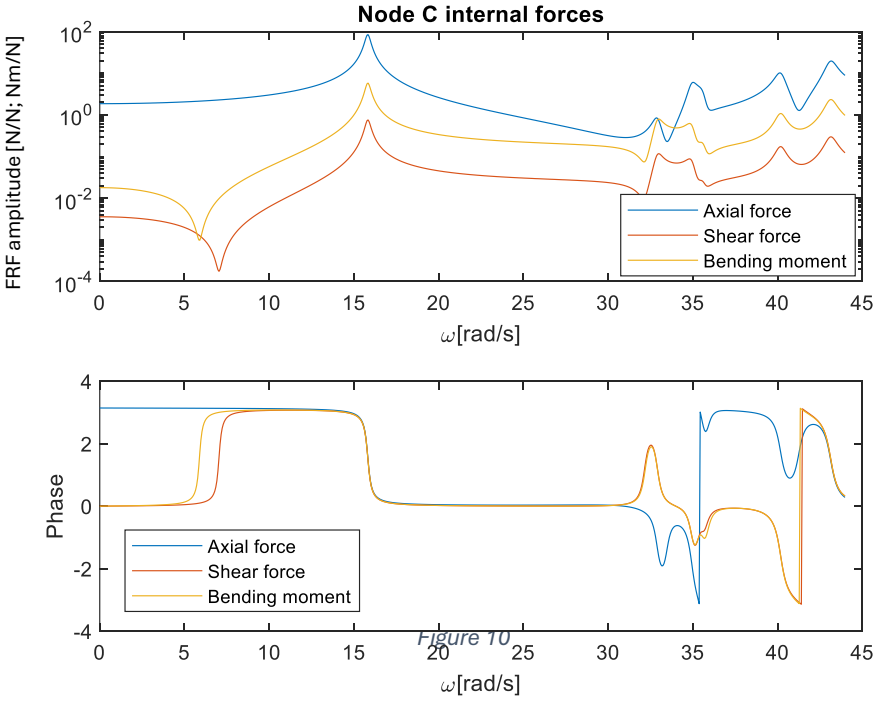

Figure 10

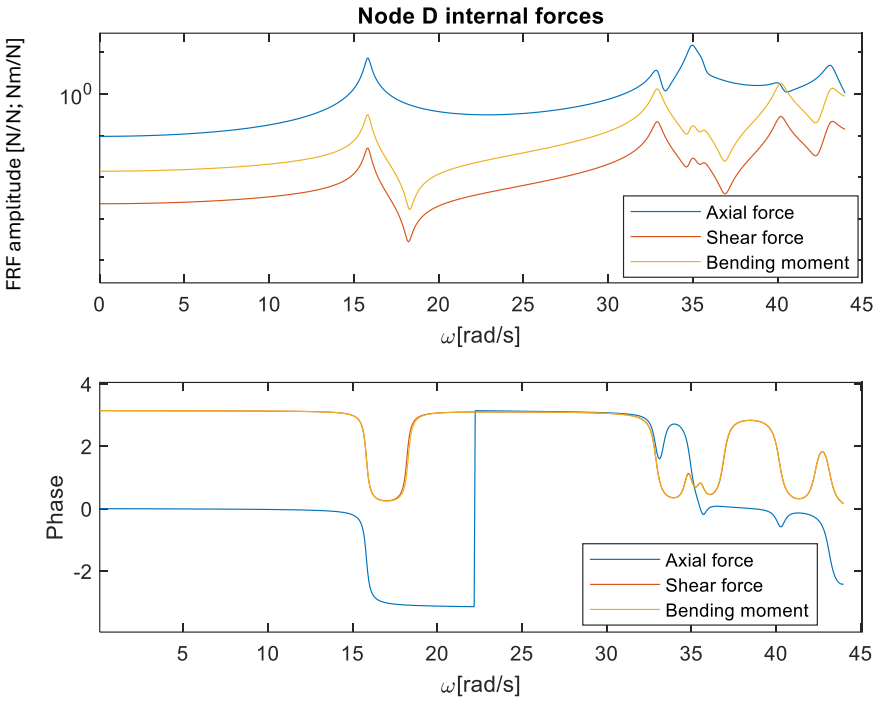

Figure 11

4.c) Constraint forces

The constraint forces are computed starting from the EoMs and considering the partition of the DoF.

$$\begin{bmatrix} [M_{FF}] & [M_{FC}] \\ [M_{CF}] & [M_{CC}] \end{bmatrix} \begin{bmatrix} \underline{\ddot{x}}_F \\ \underline{\ddot{x}}_C \end{bmatrix} + \begin{bmatrix} [C_{FF}] & [C_{FC}] \\ [C_{CF}] & [C_{CC}] \end{bmatrix} \begin{bmatrix} \underline{\dot{x}}_F \\ \underline{\dot{x}}_C \end{bmatrix} + \begin{bmatrix} [K_{FF}] & [K_{FC}] \\ [K_{CF}] & [K_{CC}] \end{bmatrix} \begin{bmatrix} \underline{x}_F \\ \underline{x}_C \end{bmatrix} = \begin{bmatrix} \underline{F}_F \\ \underline{F}_C + \underline{R} \end{bmatrix}$$

In this case there are no forces applied at the constraint, so reaction forces could be directly computed, given the matrices and the displacement already calculated.

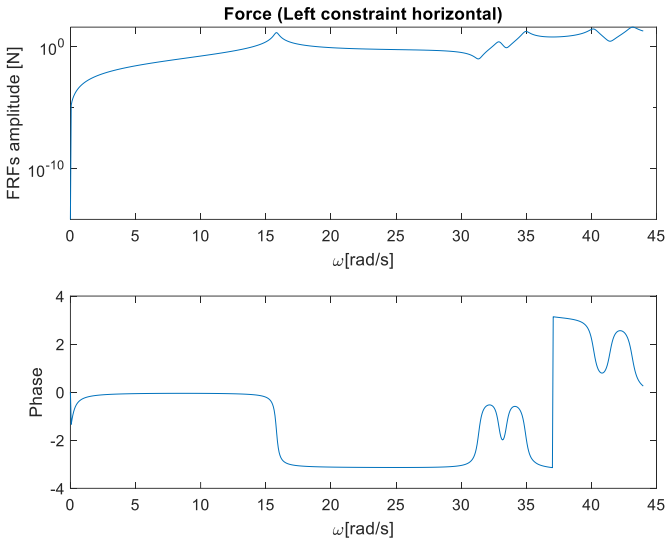

Figure 12

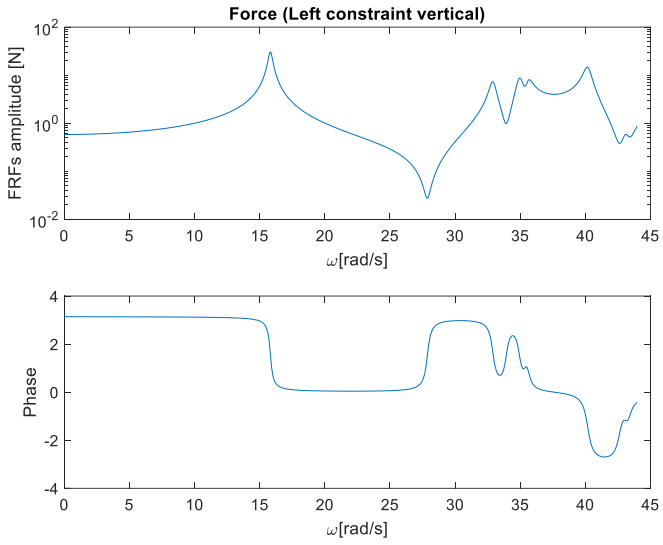

Figure 13

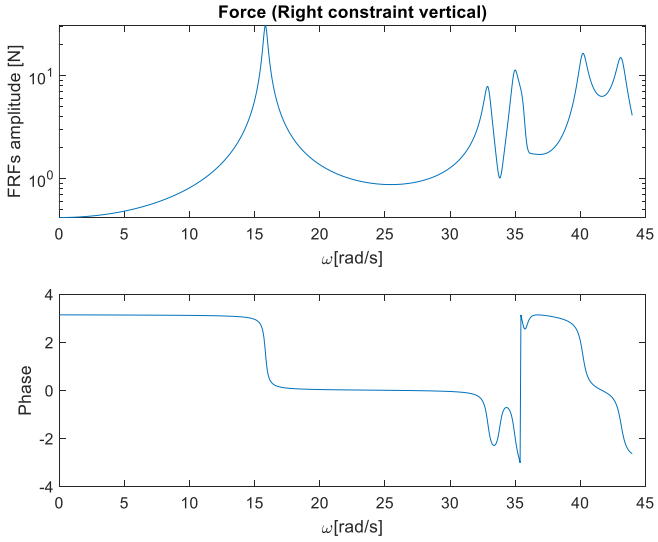

Figure 14

5) Modal superposition approach

The modal superposition approach allows us to analyze the structure by focusing only on a subset of the modes. As specified in the assignment, we concentrated on the first three modes.

We computed the matrix Φ, which is assembled with n columns corresponding to the number of modes of interest and rows equal to the total number of free degrees of freedom.

Using the matrix Φ we computed the mass, stiffness and damping modal matrices. Additionally, we calculated the generalized force vector.

$$[M_{mod}] = [\phi]'[M_{FF}][\phi]$$

$$[K_{mod}] = [\phi]'[K_{FF}][\phi]$$

$$[C_{mod}] = [\phi]'[C_{FF}][\phi]$$

$$[F_{mod}] = [\phi]'[F_0]$$

After computing the matrices, we solved the linear system to determine q_{mod} , the principal coordinates. Subsequently, we used these results to compute the physical coordinates x .

$$x = [\phi]'q_{mod}$$

From the physical coordinates, we derived the velocity and acceleration using the same procedure as in the previous section. With all the required data available, we plotted the new Frequency Response Function (FRF) as requested and compared it to the corresponding FRF obtained without using the modal approach.

The cases studied in this section focus on scenarios where the force is consistently applied on point A. The measurement positions, however, vary across the different cases considered.

Case point A

This is a collocated case where the force and the sensor are placed at the same point. In such a configuration, there is an alternation of resonance and antiresonance.

Additionally, all the modes are observable and controllable, while the third mode is not well approximated.

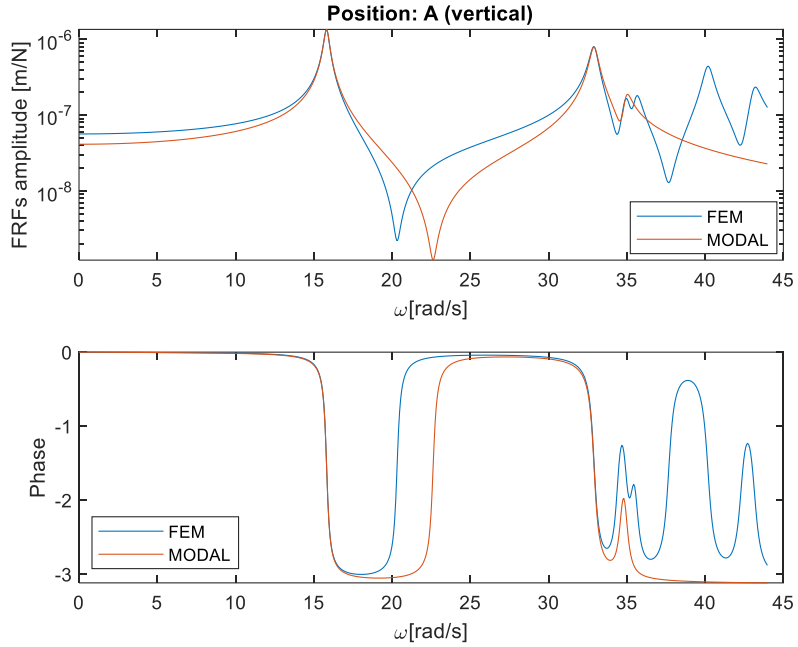

Figure 15

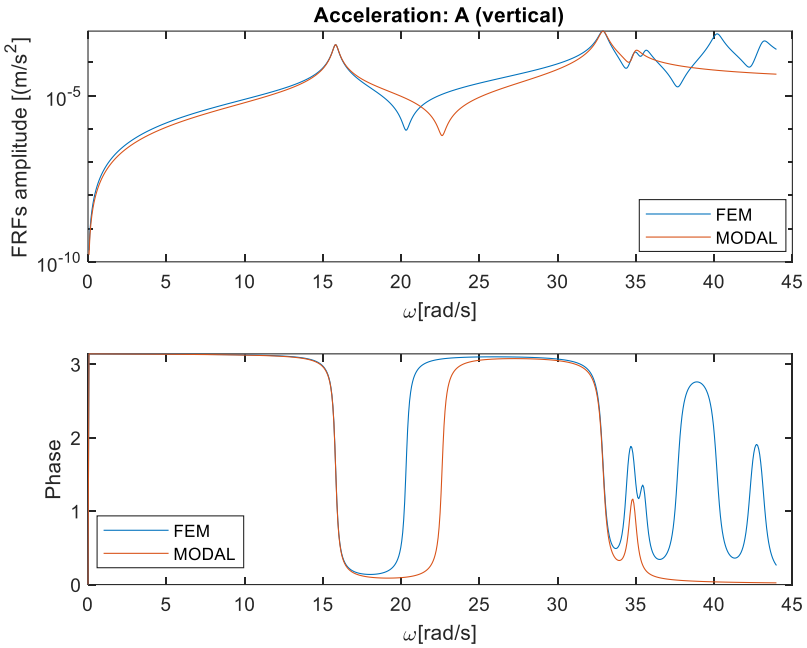

Figure 16

Case point B

In this case, the force and the sensor are positioned at two different locations. The only observable mode is the first, as point B is a node for the second mode (making it effectively non-observable) and it is also very close to a node for the third vibration mode.

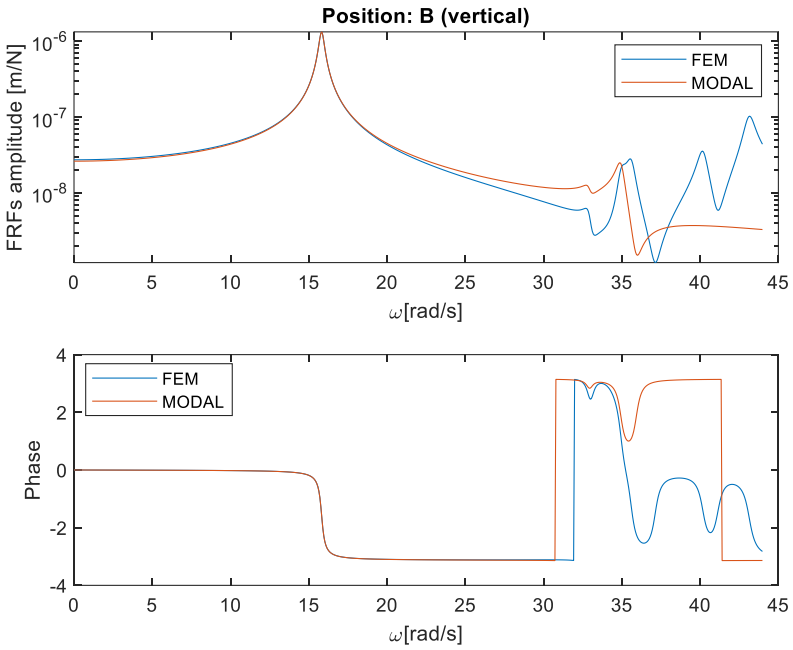

Figure 17

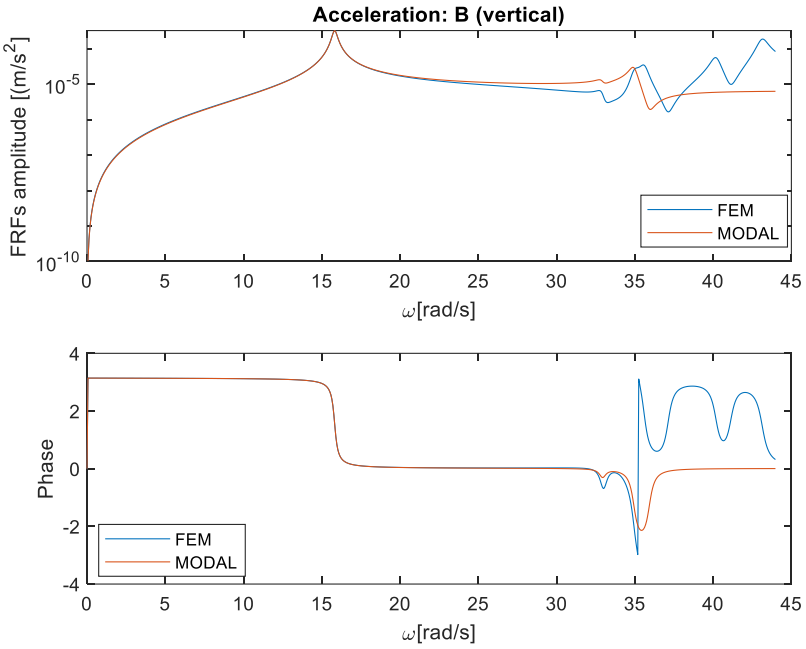

Figure 18

Case point C

In this case, the force and the sensor are positioned at two different locations. The second and the third modes are barely observable, due to the proximity with a vibration node.

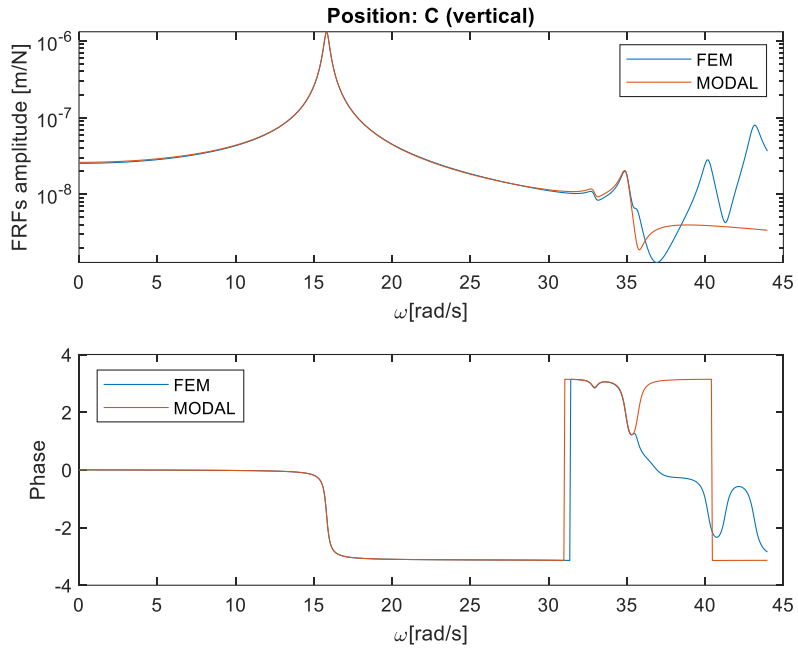

Figure 19

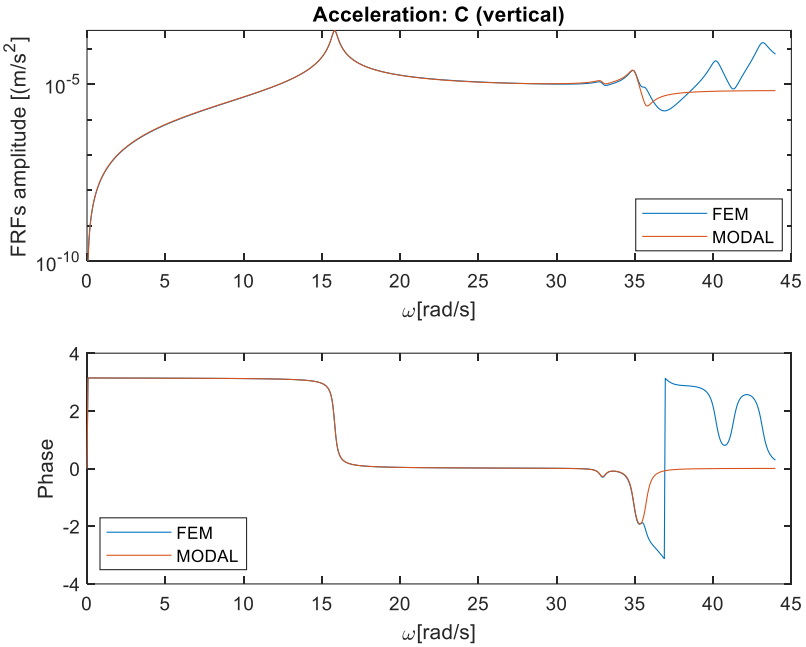

Figure 20

6) TMD

The goal is to integrate the structure with a Tuned Mass Damper to reduce the amplitude of the vibrations in point A in correspondence of the first vibration mode when unit vertical force is applied in A (same conditions as point 4). The first step of the procedure followed implies analyzing the mode shape of the bridge associated to the first natural frequency, which is reported here once again in Fig 21. (scaling factor = 10 has been used in this case).

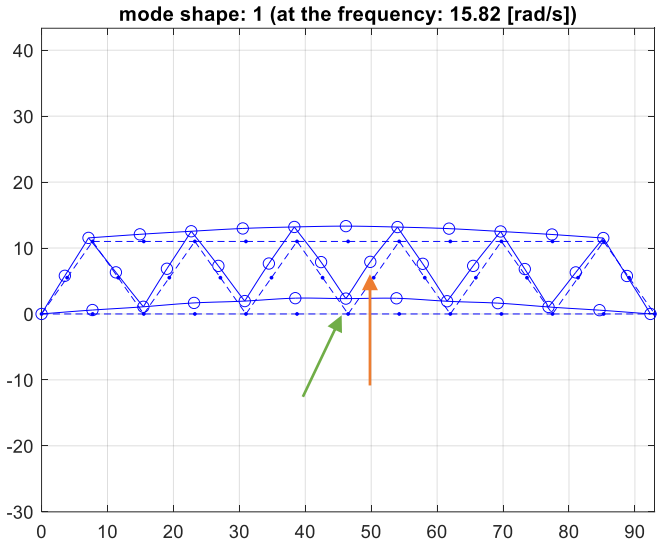

Figure 21

When discussing the positioning of the TMD, especially the connection point with the bridge, the most suitable option seems to be identifying the node with maximum vibration, which in this case is node 20. Note that this is a diagonal support element and, since the TMD is not going to be a small lightweight element, it has been decided to connect it to the main structural element of the bridge: the lower deck. Indeed, TMD has been connected to the structure in correspondence of midspan node of the lower deck (node 19) (which is very close to node 20 and experiences high vibrations as well). To introduce this new element into the structure, a new input file has been created to add an additional node, that is where the mass of the TMD is going to be placed in static condition (Fig. 22)

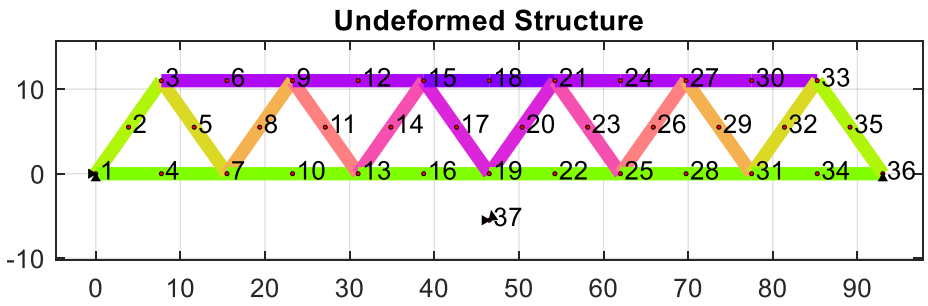

Figure 22

In the design of the TMD three parameters need to be defined: damping ratio ξ_{TMD}, mass m_{TMD} and stiffness k_{TMD}. The first one can be selected arbitrarily but the constraint given by the text must be respected ($\xi < 30\%$). On the other hand, only one between mass and stiffness can be selected arbitrarily since they are related through the expression of the natural frequency $\omega_1 = \sqrt{\frac{k}{m}}$ (ω_1 of course is the first natural frequency of the system in this case). Since the text provides a constraint on the mass (overall mass of the structure must not increase by 2%), this has been chosen as driving parameter.

To begin the identification of these parameters, two vectors have been defined with arbitrary values of mass and damping ratio; then, an iterative method has been implemented: an external loop cycles through the values in the damping ratio vector and an internal loop does the same with the mass vector. In other words, for each damping ratio, the effect of different masses has been evaluated. The following procedure describes a single iteration of the loop:

- Modification of the global mass matrix to account for the mass of the TMD in correspondence of node 37
- Modification of the global stiffness matrix to account for the one of the concentrated spring that connects the TMD with the midspan node of the lower deck:
    - Potential energy is written in the local reference system: $V = \frac{1}{2}\, k_{TMD}(x_{19}^L - x_{37}^L)^T * (x_{19}^L - x_{37}^L) = \frac{1}{2}\, k_{TMD}\left(\underline{X}_k^L\right)^T * \left[K_k^L\right] * \left(\underline{X}_k^L\right)$
    - The nodal coordinate vector in the local reference system $\underline{X}_k^L$ needs to be rewritten in the global reference system through a proper rotation matrix: $\underline{X}_k^L = [\Lambda_k] * \underline{X}_k^G$ is substituted in the previous expression. By doing this, the expression of the stiffness matrix in the global reference system is computed: $\left[K_k^G\right] = [\Lambda_k]^T * \left[K_k^L\right] * [\Lambda_k]$
    - The nodal coordinate vector in the global reference system $\underline{X}_k^G$ must be expanded to the same size as the vector that contains the nodal coordinates of all the system (of all the nodes of the system); this is performed through some proper expansion matrix: $\underline{X}_k^G = [E_k] * \underline{X}^G$ is substituted in the previous expression. The stiffness matrix that accounts for the concentrated spring of the TMD can finally be summed to the one of the system computed in the previous chapters
- Partition of the mass and stiffness matrices to compute the natural frequencies and mode shapes of the system composed of bridge + TMD (natural frequencies have slightly changed but they are still extremely close to the ones of the bridge alone)
- Damping matrix is computed at first using the Rayleigh model, the values of α, β used are the same ones computed in the previous sections
- The contribution of the concentrated damper of the TMD is introduced with the same procedure followed for the stiffness matrix
- The FRF matrix of the bridge + TMD is finally computed with the same procedure described in the previous sections

The results are being displaced below for different values of damping ratio; note that the black line represents the FRF curve of the system without the TMD and that the dashed red line represents the 85% of the maximum value of the first resonance peak:

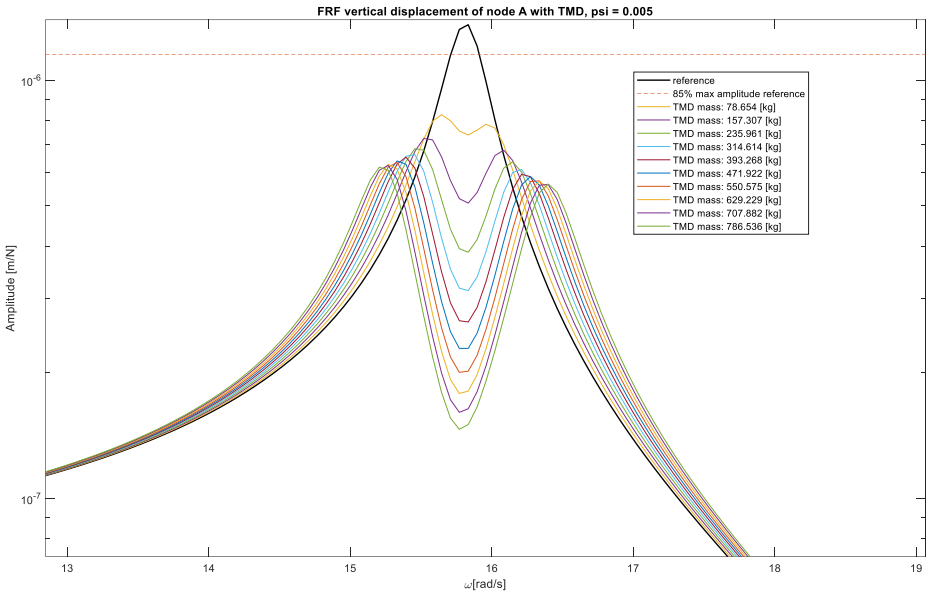

Figure 23

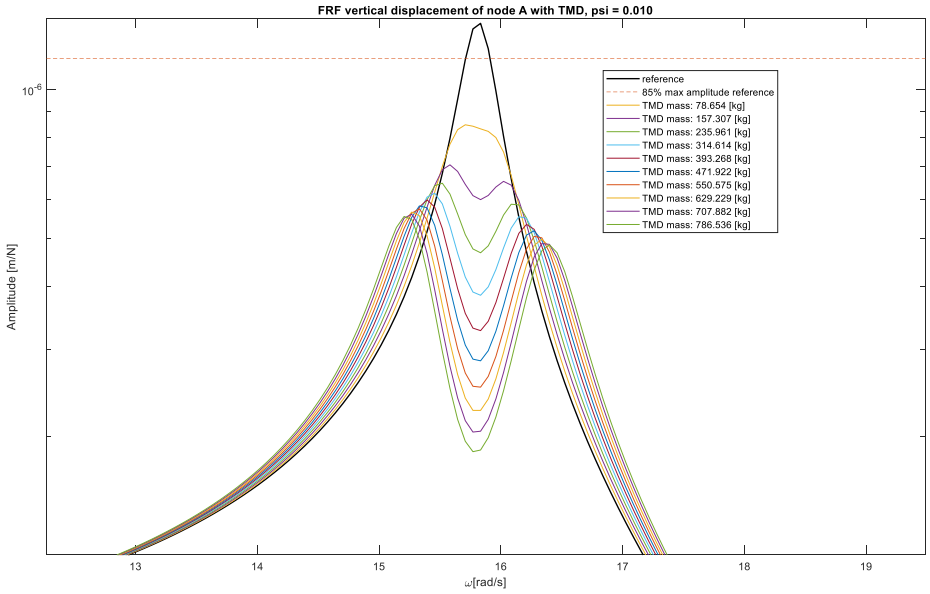

Figure 24

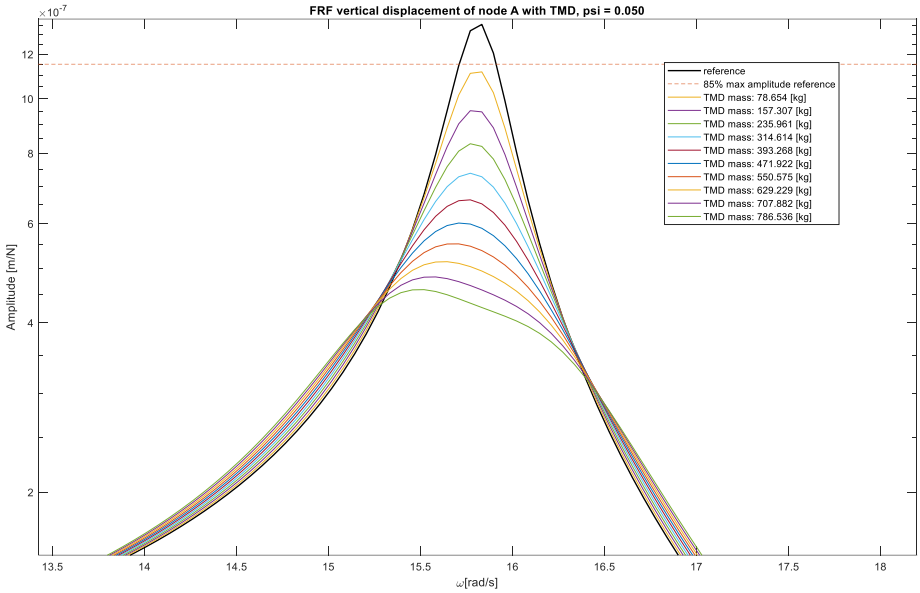

Figure 25

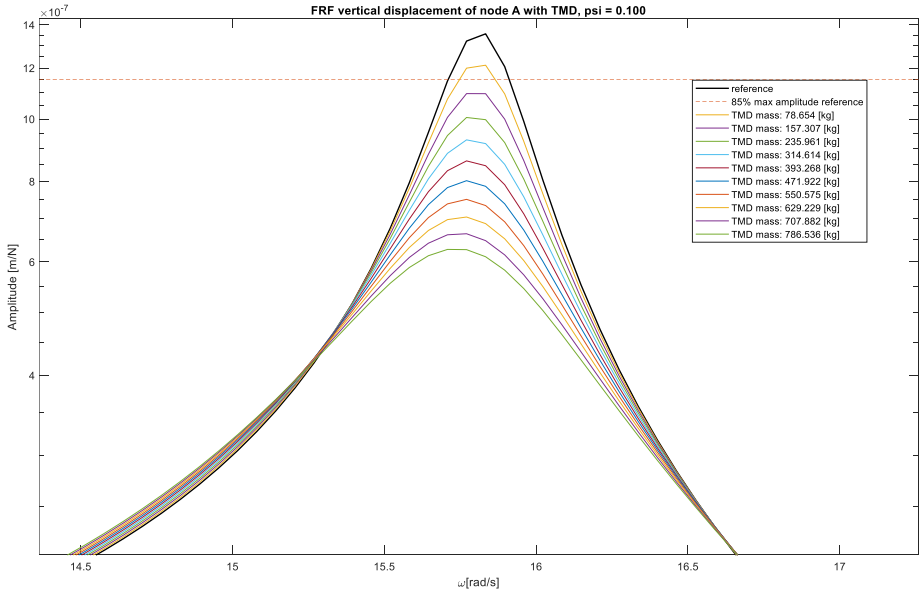

Figure 26

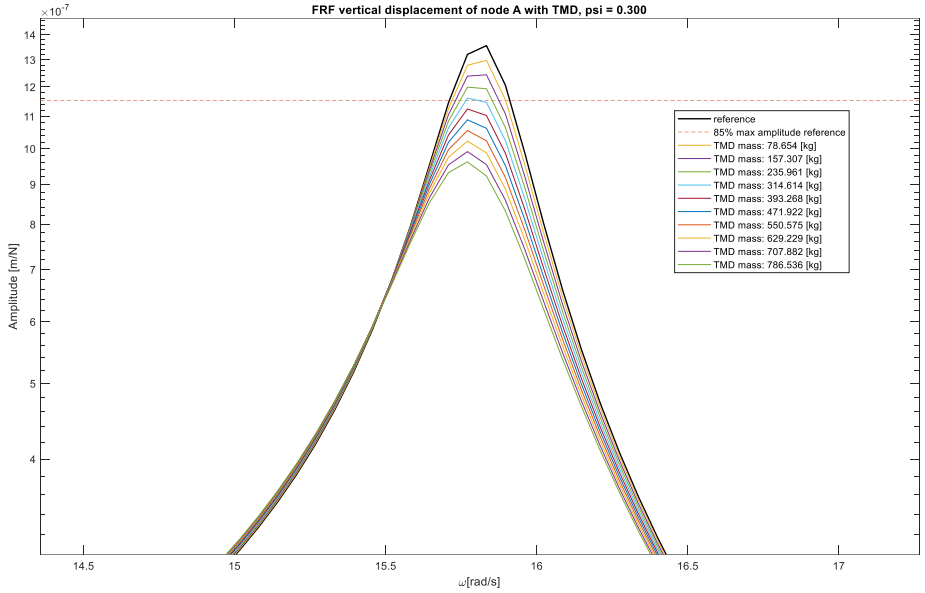

Figure 27

Some comments on the obtained results can be made:

- $\xi = 0.005$ is not a suitable value for any mass since the goal is to reduce the amplitude of the vibrations without changing the properties of the system, it not acceptable to split the main peak in two lower amplitude ones
- $\xi = 0.01$ is a suitable value only for high value of mass
- Any other combination of damping/mass is acceptable but it must be taken into account that as the mass increases, the TMD alters the dynamics of the system in a more significant way by shifting the natural frequency to lower values

In Fig. 28, two mode shapes have been reported for two corresponding combinations of stiffness and mass (same scaling factor = 10). If compared to the first mode shape of the bridge alone reported previously, the positive effect of the TMD in reducing the amplitude of the vibrations can be observed.

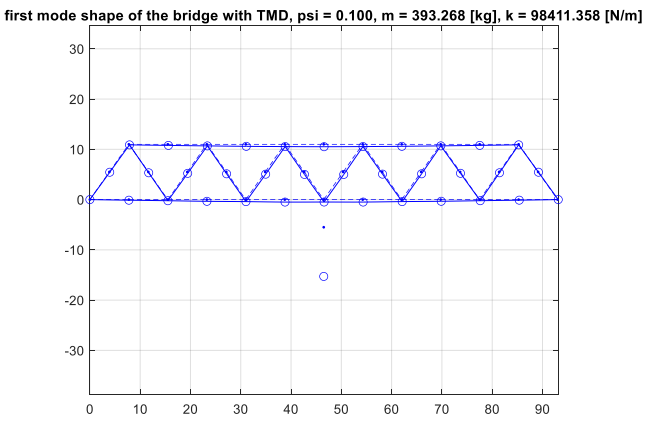

Figure 28a

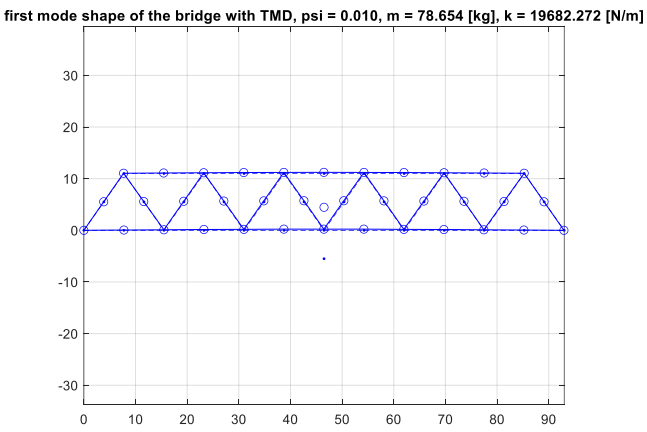

Figure 28b

7) Static response of the structure

7.1) Procedure 1

7.1.a) Lower deck weight only

To compute the static deflection associated to the deck weight we identified the indices of the y-coordinates of the deck nodes using the IDB matrix. Subsequently, we constructed a force vector (F_deck_m) whose elements were non-zero only at the points corresponding to the coordinates identified in the IDB matrix. The force vector was computed as:

$$F\_deck\_m = M \cdot gacc\_v$$

where gacc_v is a vector with values equal to -9.81at the points corresponding to the coordinates identified with the IDB matrix.

Finally, we computed the position values by solving the simple linear system:

$$X\_pos\_deck\_v = KFF \backslash F\_deck\_m(1: n\_cfree)$$

X_pos_deck_v is the vector that represents the static response of the system, considering just the deck weight.

The maximum deflection was computed using the **max** function on the absolute values (**abs**) of the position vector, obtaining a maximum deflection of **0.037 m** at node 22.

7.1.b) Whole bridge weight

The same procedure was followed to compute the static response considering the weight of the entire bridge. In this case, we identified the y-coordinates of all the nodes, not just the deck nodes, using the IDB matrix

The maximum deflection is **0.048 m** at node 17.

7.2) Procedure 2

7.2.a) Lower deck weight only

The starting point to compute the static deflection associated to the deck weight is to assume each FE of the lower deck to be excited with a constant distributed load equal to the product of the mass per unit length and -g. The goal is to compute the work equivalent nodal forces that excite the structure and to analyse the response in static conditions.

The very first step of the procedure needs to be, clearly, the identification of finite elements that build up the lower deck; this builds up a vector of twelve elements. The following procedure has been performed for each i element of this vector.

1) Computation of the constant load $p = -9.81 * m_i$; it is a weight force per unit length, and it is directed along the y axis only
2) The expression of the virtual work of the distributed load has been considered:

$$\delta W_{ext,i} = \left(\delta \underline{x}_i^L\right)^T \left[\int_0^{L_i} \underline{f_u}(\xi) p_x(\xi) d\xi + \int_0^{L_i} \underline{f_w}(\xi) p_y(\xi) d\xi\right]$$

As mentioned before, the distributed load only has component along y: $p_y = p;\ p_x = 0$

3) The resolution of the integral provides as result the work equivalent nodal forces vector acting on finite element i in the local reference system:

$$\underline{F}_i^L = p_0 \int_0^{L_i} \begin{bmatrix} 0 \\ 2\frac{\xi^3}{L_i^3} - 3\frac{\xi^2}{L_i^2} + 1 \\ \frac{\xi^3}{L_i^2} - 2\frac{\xi^2}{L_i} + \xi \\ 0 \\ -2\frac{\xi^3}{L_i^3} + 3\frac{\xi^2}{L_i^2} \\ \frac{\xi^3}{L_i^2} - \frac{\xi^2}{L_i} \end{bmatrix} d\xi = p_0 \begin{bmatrix} 0 \\ \frac{L_i}{2} \\ \frac{L_i^2}{12} \\ 0 \\ \frac{L_i}{2} \\ -\frac{L_i^2}{12} \end{bmatrix}$$

4) The force vector needs to be rewritten in global reference system through a proper rotation matrix: $\underline{F}_i^G = [\Lambda_k]\underline{F}_i^L$
5) The force vector needs to be expanded to the same size as the global mass and stiffness matrices (size, 3N x 3N), this is performed through a proper expansion matrix. In addition, the contribution of each finite element is summed in a vector: $\underline{F}^G = \sum_i [E_i]^T \underline{F}_i^G$

After having computed and summed all the contributions of the lower deck elements to the equivalent nodal force vector, the static deflection can finally be computed. This is performed by considering the free-free partition of the matrices and of the force vector (the distributed load is an active force not applied on the constraints, see slide 32 lez. 08):

$$[M_F F]\underline{\ddot{x}}_F + [C_{FF}]\underline{\dot{x}}_F + [K_{FF}]\underline{x}_F = \underline{F}_F^G$$

Recalling that in static conditions $\underline{\ddot{x}}_F = 0$; $\underline{\dot{x}}_F = 0$, the static deflection is given by $\underline{x}_F = [K_{FF}]^{-1}\underline{F}_F^G$. The deflection of the bridge under the effect of the weight of the lower deck only is reported in Fig.29 (scaling factor = 40); note that the maximum deflection computed is **0.036 m** (node 16, highlighted in green).

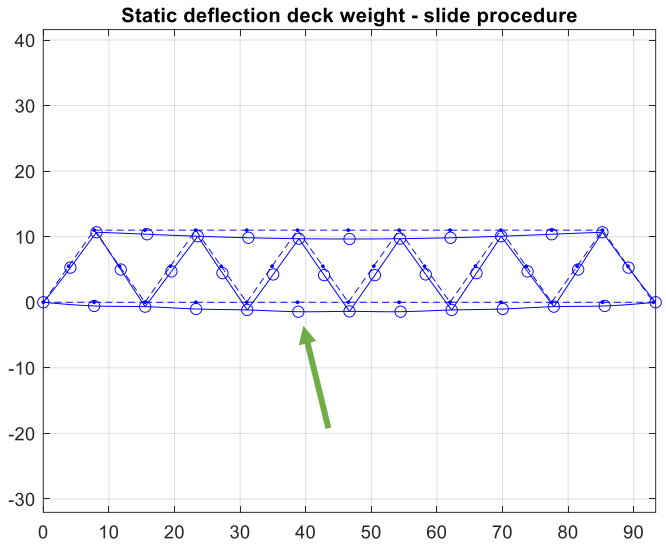

Figure 29

7.2.b) Whole bridge weight

The exact same procedure described previously has been used, the only difference is that in this case all the FE of the bridge have been considered and not only the ones of the lower deck. The deflection of the bridge under the effect of the weight of whole structure is reported in Fig.30 (scaling factor = 40); note that the maximum deflection computed is **0.048 m** (node 17, highlighted in green).

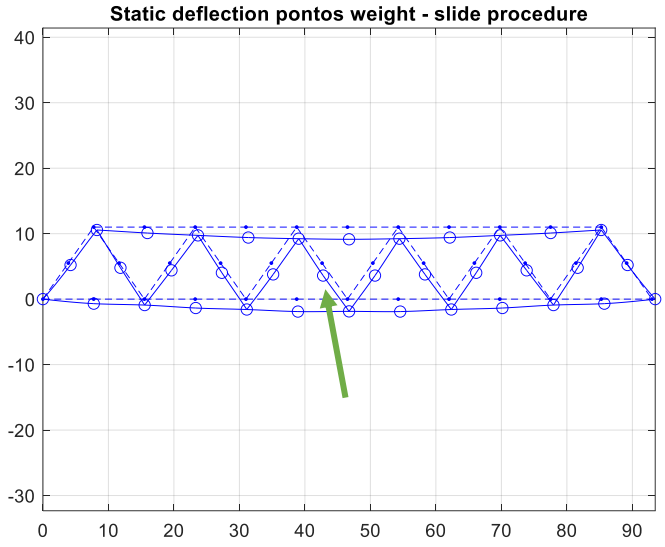

Figure 30

8) Critical velocities

To calculate the critical velocities for the first two vibration modes, we determined the required frequencies by selecting the first and second natural frequencies of the structure; then we computed them through the following formula:

$$V_{ik} = \frac{f_i d}{k}$$

In this context, f represents the natural frequencies of the structure, d denotes the spacing between consecutive loads, and k corresponds to the k-th harmonic component of the generalized force. The most critical scenarios occur in the first two to three vibration modes and for the lowest harmonic values (k≤3). Therefore, critical velocities were calculated by varying k from 1 to 3.

The results are

	V_1(km/h)	V_2(km/h)
k = 1	249.249	518.473
k = 2	124.624	259.236
k = 3	83.083	172.824